Vol 12 No 11, November 2003
1009-1963/2003/12(11)/1305-05

Chinese Physics

© 2003 Chin. Phys. Soc.
and IOP Publishing Ltd

Domain structures of $Nd_{13}Fe_{80}B_7$ magnets during HDDR process*

Zhang Zhen-Rong(张臻蓉)[a], Pang Zhi-Yong(庞智勇)[b], Zhao Yi-Min(赵义敏)[c], Zhang Zheng-Yi(张正义)[c], Han Sheng-Hao(韩圣浩)[b], and Han Bao-Shan(韩宝善)[a]†

[a] *State Key Laboratory of Magnetism, Institute of Physics, and Center of Condensed Matter Physics, Chinese Academy of Sciences, Beijing* 100080, *China*

[b] *School of Physics and Microelectronics, State Key Laboratory of Crystal Materials, Shandong University, Jinan* 250100, *China*

[c] *Institute of Materials, University of Science and Technology Beijing, Beijing* 100083, *China*

(Received 20 May 2003; revised manuscript received 8 August 2003)

The domain structures of $Nd_{13}Fe_{80}B_7$ alloy at different stages of the HDDR process have been revealed using a magnetic force microscope. In the as-cast samples, the columnar crystals with easy axis perpendicular to one another are clearly characterized by their different domain structures. For the insufficient and sufficient HD treatment, an obvious change of domain structure occurs, which is related to the variation of composition and crystalline microstructure during the HD process. And for the samples after sufficient DR processing, it is confirmed that the configuration of the columnar crystals is retained by the detected domain structures.

Keywords: magnetic domain structure, Nd-Fe-B, HDDR, magnetic force microscope (MFM)
PACC: 7560C, 7550B, 8140R, 0779

1. Introduction

The hydrogenation, disproportionation, desorption and recombination (HDDR) process has been developed and has attracted attention as a method of producing anisotropic Nd-Fe-B-based alloy powders.[1] In the process, Nd-Fe-B phase disproportionates to NdH_2, α-Fe and Fe_2B at elevated temperature in the presence of hydrogen, and then in a subsequent dehydrogenation process, the disproportionated mixture recombines to give a Nd-Fe-B compound, which consists of fine anisotropic powders in high quality. Based on the study of the microcrystalline structure, some models have been proposed for the mechanism of developing anisotropy in the HDDR-processed powder materials.[2−8] However, until now very few works have been focused on the magnetic domain structure in the HDDR process. It is well known that magnetic microstructure is closely related to the crystalline microstructure and to the magnetic properties of magnetic materials, therefore, the domain structure variation of the $Nd_{13}Fe_{80}B_7$ magnets at different stages of the HDDR process is worth studying using the magnetic force microscope (MFM).

2. Experimental

The $Nd_{13}Fe_{80}B_7$ alloy was induction melted and cast at 1500–1550°C in an Ar atmosphere. The ingots were subsequently homogenized at 1050°C for 24h and then cooled down to room temperature. Parallel to the columnar crystals, ingots were cut into plates with a thickness of about 1mm. They were heated in vacuum to 800°C, and then pure hydrogen was introduced into the heating chamber. The samples were maintained at constant temperature and underwent the hydrogenation and disproportionation (HD) process for 180min. The temperature was then increased to 850°C for desorption and recombination process (DR) for 120min. To observe the variation of domain structure during the HD process in detail, the HD reaction was interrupted by evacuating and cooling rapidly down to room temperature after 15 and 180min. Analysis of phase composition and structure

*Project supported by the National Natural Science Foundation of China (Grant No 10074081) and by the National Key Basic Research and Development Programme of China (Grant No 2001CB610504).

†bhan@aphy.iphy.ac.cn

at different stages of HDDR process was performed by means of x-ray diffraction (XRD). The samples were examined using a Siemens D5000 x-ray diffractometer with Cu-$K\alpha$ radiation. And magnetic properties were measured using an LDJ9600 vibrating sample magnetometer (VSM) at a field of 1592kAm^{-1}. In our experiments, the detection of magnetic domain structure and topographic feature of the samples was performed by a NanoScope IIIa-D3000 MFM in Tapping/Lift modes. The magnetic tips used were microfabricated Si cantilevers with a pyramidal tip coated with magnetic Co-Cr thin film about 40nm thick and magnetized downward prior to imaging. The tip lift-height was in the range of 30–100nm. The oscillation frequency of the tip was about 67kHz. Before MFM experiments, the samples were ground and polished using standard metallurgical procedures, followed by vacuum annealing to remove the stress built up in the sample surface layer during the procedures. Because the surface contamination took place in HD and DR treatment, the samples were re-processed again for MFM detection.

3. Results and discussion

To confirm the validity of our experiment, we first measured the magnetic properties of the bonded $Nd_{13}Fe_{80}B_7$ magnets made of the anisotropic powders produced by the HDDR process described above. The magnets exhibit intrinsic coercivity H_{cj} of 636kAm^{-1} and energy product $(BH)_m$ of 82.6kJ/m^3 ($\sim$10.5MGOe). We also found that the residual induction B_r along the alignment direction is 0.77T, which is much higher than 0.34T along the transverse direction, indicating a significant anisotropy of the magnets. The above data show the effectiveness of the HDDR process used.

Secondly, the magnetic properties, such as intrinsic coercivity H_{cj}, magnetic polarization strength J, and residual polarization strength J_r of the four typical samples tested at different HDDR stages were also measured and listed in Table 1. It can be seen that H_{cj} and J_r are dramatically increased from 10.7kAm^{-1} and 0.020T for the as-cast sample to 375kAm^{-1} and 0.641T of the sample after DR, respectively, while J_{1592} (measured at the field of 1592kAm^{-1}) is almost unchanged, showing the material became hard magnetic. It should be noted that the field of 1592kAm^{-1} can saturate both the samples of 15min HD and 180min HD, but is far from saturating the as-cast sample and the sample after 120min DR.

Table 1. The intrinsic coercivity H_{cj}, the magnetic polarization J_{1593} measured at a field of 1592kAm^{-1}, and the residual polarization J_r of the typical as-cast samples used in MFM detection and their properties after suffering 15 min HD, 180 min HD, and 120 min DR treatment, respectively.

Samples	H_{cj}/(kA/m)	J_{1592}/T	J_r/T
As-cast (unsaturated)	10.7	1.138	0.020
After 15 min HD	56.2	1.465	0.170
After 180 min HD	10.8	1.597	0.169
After DR (120 min) (unsaturated)	375	1.180	0.641

The analysis of XRD confirmed that the as-cast $Nd_{13}Fe_{80}B_7$ alloy sample possesses perfect Nd-Fe-B phase. Figure 1 shows three typical 80μm$\times$80μm magnetic force images captured at different areas. Figure 1(a) clearly shows the columnar crystals with easy axes perpendicular to one another. The plate domain pattern is presented by the crystals with in-plane easy axis (c axis) in the middle of the image, while the corrugation and spike domain pattern in the upper and lower parts of the image indicates that the easy axis of the crystals is normal to the surface. From many images captured with a mixture of domain patterns, we found that the size of the columnar crystals is of the size of 25–35μm. Except for the mixture of the two patterns, single plate domain pattern and single corrugation and spike domain pattern are presented in Fig.1(b) and Fig.1(c), respectively. Besides, in the images, we can also see that at the boundary of the crystals, non-magnetic Nd -rich phase exists as white areas without any domain pattern in them.

From the images of Fig.1, we notice that the c axis of the column-like crystals is either in the plane of, or normal to the sample surface. In fact, this feature is associated with the tetragonal structure of Nd-Fe-B.[9] In the crystal cells of Nd-Fe-B, the atoms of Fe, Nd and B have laminate distribution along c axis, therefore, during growth, it is faster to grow along a axis, but much slower along c axis, leading to the formation of columnar crystals in the ingots. Moreover, as we know, there are two completely equivalent a axis in Nd-Fe-B crystal cells and for Nd-Fe-B crystals, the two easy growth directions, [410] and [411], are also symmetrical and perpendicular to one another, leading to the existence of 90° phase difference between the column-like crystals growing along [410] and [411] directions.

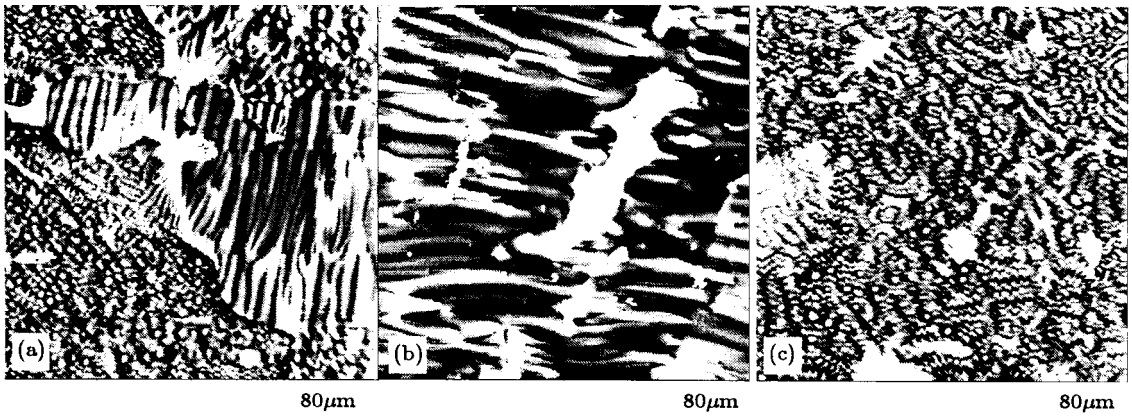


Fig.1. Typical magnetic force images of the as-cast $Nd_{13}Fe_{80}B_7$ alloy captured at different areas. (z range=50°, lift height of the tip=100nm).

Using the roughness analysis, for Figs.1(a),1(b) and 1(c) the average of their root mean-square value of phase shift, $(RMS)_{\Delta\phi}$, was 8.6°. In fact, $(RMS)_{\Delta\phi}$ can be used to represent the contrast of magnetic force images because the phase shift $\Delta\varphi$ of tip oscillation is directly proportional to the second derivative of the vertical component H_z of the stray fields emerged from sample surface.[10] Therefore, generally speaking, phase shift $\Delta\varphi$ can give an indication of the effective magnetic moment of the sample. Thus, the relatively high $(RMS)_{\Delta\phi}$ value accounts for the higher saturation magnetization of the as-cast sample.

For the sample after the HD treatment for 15min, three typical magnetic force images are shown in Fig.2. Among them, the two images, Fig.2(a) and 2(b) with 20 μm and 40μm scan size, respectively, were captured at the same area, but Fig.1(c) with 80μm scan size was captured at another spot.

As shown in Fig.2, the contrast of the images becomes much weaker compared with the as-cast sample under the same tip lift-height (100nm) (note that the z range of Fig.2 is only 10°, but that of Fig.1 is as high as 40°). In fact, the $(RMS)_{\Delta\phi}$ value of Fig.2(c) was only 1.0°. Moreover, the domain structures of Fig.2 are characteristic of inhomogeneous distribution of the areas with higher or lower contrast. In the lower contrast areas, the nonmagnetic phase contain the bright-dark magnetic spots with weak contrast.

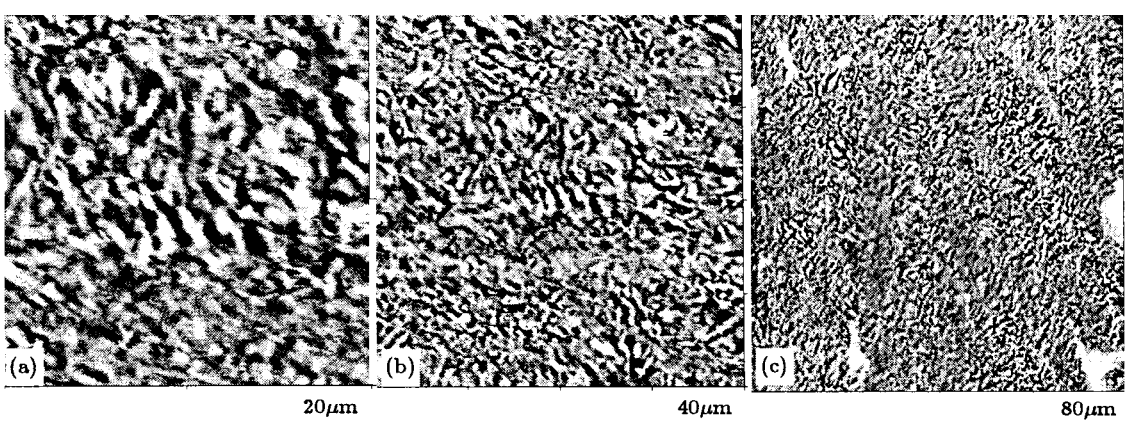


Fig.2. Typical magnetic force images of the $Nd_{13}Fe_{80}B_7$ alloy after 15 min HD treatment (z range=10°, lift height of the tip=100nm).

Based on the results of metallurgical analysis[9,11,12] and our XRD analysis, we believe that the nonmagnetic phase is NdH_2 and the weak bright-dark spots inside result mainly from soft magnetic α-Fe phase because α-Fe phase appears as tiny plates in random directions although it possess high magnetization. Besides, in the XRD spectrum, additional diffraction peaks of Nd-Fe-B phase were identified, thus in the higher contrast areas, the irregular stripe domains with narrower domain width should be the contribution of the survivals of $Nd_2Fe_{14}B$ phase, which were not disproportionated yet after the short HD pro-

cess. The remains of $Nd_2Fe_{14}B$ phase have smaller crystal size and irregular shape, and are randomly distributed because only a part of as-cast $Nd_{13}Fe_{80}B_7$ alloy was disproportionated and the insufficient disproportionation process occurred randomly. The above fact manifests that the time of 15min is not enough for a complete HD reaction, and Fig.2 just illustrates a transition state of the HD stage.

As shown in Table 1, after 15min HD, the sample's J_{1593} is 1.465T, which is only a little smaller than that of the normal $Nd_2Fe_{14}B$ ($\sim$1.61T). This is due to the coexistence of magnetic α-Fe and non-magnetic NdH_2, and the J_s value of α-Fe $\sim$2.16T, which is much higher than that of $Nd_2Fe_{14}B$. However, the corresponding $(RMS)_{\Delta\phi}$ value of Fig.2 was largely decreased, as described above. The reason is that after 15min HD process, the magnetic phases in the sample were much smaller and fewer, and distributed randomly, leading to much weaker stray fields emerging from the sample surface and then very low value of $(RMS)_{\Delta\phi}$.

Typical topographic and magnetic force images ($40\mu m \times 40\mu m$) of the $Nd_{13}Fe_{80}B_7$ sample after 180min HD treatment are shown in Fig.3. It is seen that after 180min HD, areas with higher contrast almost disappeared, indicating the HD reaction was almost complete, which was also confirmed by the XRD analysis. As more clearly shown in the typical $5\mu m \times 5\mu m$ topographic image Fig.4(a), there is a more homogeneous distribution of spherical grains in scale of about 250nm. Meanwhile, in the corresponding magnetic force image Fig.4(b), there are non-magnetic phase NdH_2 without contrast blended with bright-dark magnetic spots (α-Fe and Fe_2B). Therefore, we believe that the spherical grains in Fig.4(a) are NdH_2, α-Fe and Fe_2B grains formed after a complete HD process.[13] Moreover, as shown in Table 1, after the HD treated for 180min, the J_{1593} value of the sample is quite close to that of the normal $Nd_2Fe_{14}B$ ($\sim$1.61T) due to the entire disproportionation of the residual $Nd_{13}Fe_{80}B_7$ phase remained after the 15min HD and the corresponding value of H_{cj} is decreased largely due to the formation of soft magnetic α-Fe and Fe_2B.

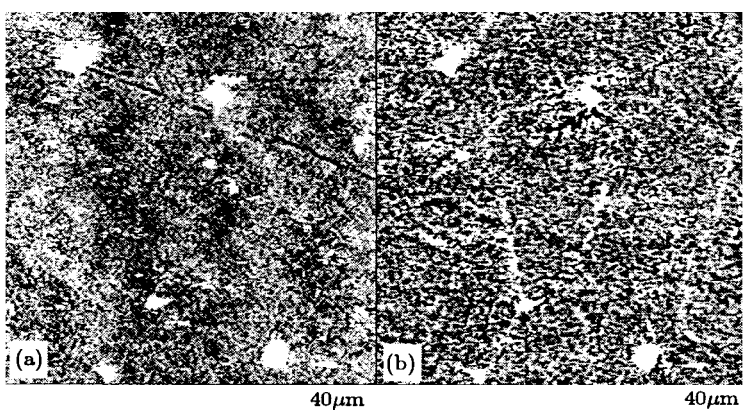


Fig.3. Typical topographic image (a) and magnetic force image (b) of the $Nd_{13}Fe_{80}B_7$ alloy after 180 min HD treatment (z range=80nm for (a); z range 10° and lift height of the tip=30nm for (b)).

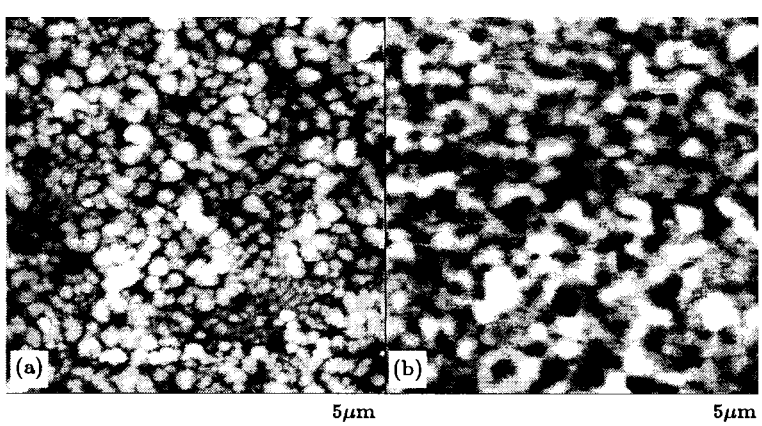


Fig.4. Typical small scale topographic image (a) and magnetic force image (b) of the $Nd_{13}Fe_{80}B_7$ alloy after 180 min HD treatment. (z range=50nm for (a); z range 15° and lift height of the tip=30nm for (b)).

For the $Nd_{13}Fe_{80}B_7$ alloy after 180min DR reaction, XRD analysis shows that the sample was in full $Nd_2Fe_{14}B$ phase, indicating that the whole HDDR process is completed. For the sample, three typical $80\mu m \times 80\mu m$ magnetic force images are shown in Fig.5. It is worthwhile to note that Fig.5(a) looks like "returning" to Fig.1(a), and Fig.5(b) and Fig.5(c) are also similar to Fig.1(b) and Fig.1(c), respectively. Taking Fig.5(a) as an example, the columnar crystals become clear again, and there exist "plate domains" with in-plane magnetization in a large part of the image, and "corrugation and spike domains" with perpendicular magnetization at the upper left corner. This fact indicates that in the same areas, countless resultant micro-crystals possess almost the same magnetization direction. However, because the resultant micro-crystals after the HDDR process are much finer, the domains becomes blurry and smaller in scale. The above fact verifies that the recombined micro-crystals originating from the same columnar crystals retain the configuration of the previous columnar crystals. Meanwhile the average $(RMS)_{\Delta\phi}$ value of Figs.5(a), 5(b) and 5(c) is increased to 8.1°, only a little smaller than 8.6° of Figs.1(a), 1(b) and 1(c). This fact reflects the identical collocation of the recombined micro-crystals, resulting in a tremendous increase of the stray fields. In fact, it is the fining down of the as-cast $Nd_{13}Fe_{80}B_7$ alloy crystals that make it possible to tremendously increase the intrinsic coercivity and hence the energy product of the recombined sample, as shown in Table 1.

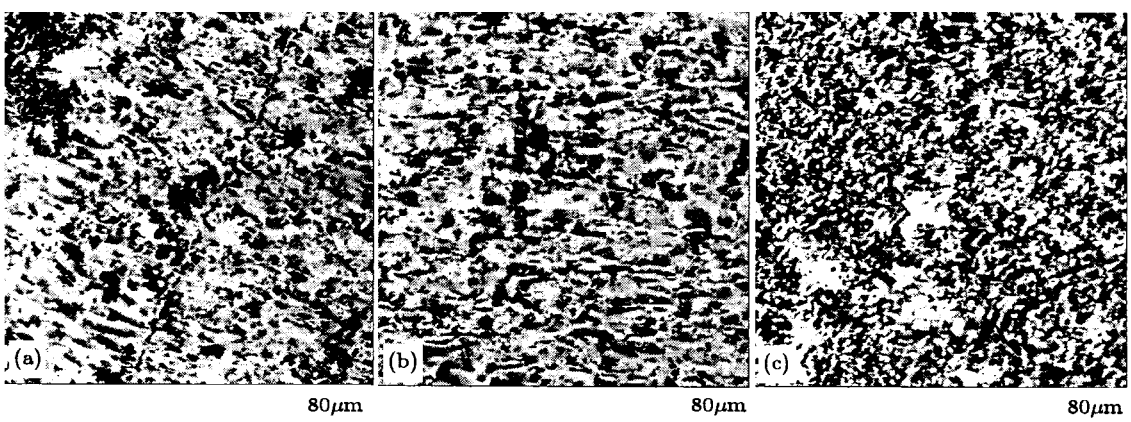


Fig.5. Typical magnetic force images of the $Nd_{13}Fe_{80}B_7$ alloy after 120 min DR treatment (z range=50°, lift height of the tip=100nm).

4. Conclusions

The HDDR process of $Nd_{13}Fe_{80}B_7$ alloy has been studied using a magnetic force microscope (MFM). From the point of view of magnetic microstructure, some details of the HDDR process, such as the variation of domain structures at different HDDR stages and the correlation between magnetic and crystalline microstructures during the HDDR process have been revealed. Combined with XRD analysis and magnetic measurements, the features of the domain structures were explained.

References

[1] McGuiness P J *et al* 1992 *IEEE Trans. Magn.* **28** 2160
[2] Nakayama R *et al* 1993 *J. Alloy Compound* **193** 259
[3] Tomida T *et al* 1997 *J. Appl. Phys.* **81** 7170
[4] Uehara M *et al* 1995 *IEEE Trans. Magn.* **31** 3632
[5] Bushow K H J 1994 *IEEE Trans. Magn.* **30** 565
[6] Actis F A *et al* 1996 14th *Int. Workshop on RE Magnet & Their Applications, Dresden* Germany, Sao Paulo, Brazil, p174
[7] Rupp B *et al* 1988 *J. Mater. Sci.* **23** 133
[8] Gutfleisch O *et al* 2000 *J. Magn. Magn. Mater.* **210** L5
[9] He Y Q *et al* 1999 *Acta Metall. Sin.* **3** 271 (in Chinese)
[10] Babcock K *et al* 1995 *Mat. Res. Soc. Symp.* **355** 311
[11] Matzinger M *et al* 1995 *IEEE Transs. Magn.* **31** 3635
[12] Guttleisch O *et al* 1995 *J. Magn. Magn. Mater.* **147** 320
[13] Guttleisch O *et al* 1994 *J. Alloy Comp.* **204** L21